Journal of Hydrology, 2022 – Accepted paper – https://doi.org/10.1016/j.jhydrol.2022.127485

Flood damage functions based on a single physics- and data-based impact parameter that jointly accounts for water depth and velocity

Tommaso Lazzarin[a], Daniele P. Viero[a], Daniela Molinari[b], Francesco Ballio[b], Andrea Defina[a]

[a] Department of Civil, Environmental and Architectural Engineering, University of Padova, Italy.

[b] Department of Civil and Environmental Engineering, Politecnico di Milano, Italy.

Corresponding author: Tommaso Lazzarin (tommaso.lazzarin@phd.unipd.it)

Highlights

- A non-dimensional physics- and data-based parameter is introduced to measure flood hazard
- It accounts for flow depth and velocity and encompasses the concepts of energy and momentum
- It enhances traditional models and allows reconciling previous results in a unique general form
- Relative damage functions are obtained using a mixed deterministic-probabilistic approach
- The effectiveness of the method is proved by application to people, vehicles, and buildings

Abstract

Direct flood damage is commonly assessed using damage models (i.e. vulnerability functions and fragility curves), which describe the relationship between hazard, vulnerability, and the (probability of) damage for items exposed to floods. In this paper, we introduce a non-dimensional impact parameter that, according to the physics of damage mechanisms and/or tuned on field or lab data, combines water depth and flow velocity in a general and flexible form. We then suggest a general approach to assess relative damage functions for items of different nature, subject to either *progressive* or *on-off* damage processes. The proposed method enhances traditional tools that use inundation depth as the main (or only) explicative variable, and allows recasting the results from previous studies in an elegant, flexible and unique form. Compared to multivariate models that link flow variables to damage directly, the physics-based approach allows for an intelligible assessment of flood hazard and the associated damage, even in case of scarce or sparse data. The proposed impact parameter and the related procedure to assess the relative damage functions are applied to different kinds of exposed items (people, vehicles, and buildings), demonstrating the general applicability and validity of the proposed method.

Keywords

Damage; Flood; Hazard; Vulnerability; Vulnerability function; Flood risk.

1 Introduction

Flood damage assessment is a fundamental step and a key information basis in any deliberation on flood risk management, being it related to long-term mitigation measures or to the emergency phase (see, e.g., the European Floods Directive). Two kinds of tools are generally used to assess direct flood damage (Pregnolato et al., 2015; Fuchs et al., 2019a). The standard tool is represented by vulnerability curves relating hazard, exposure, and vulnerability to the damage, usually expressed in relative terms, on a scale ranging from 0 = no damage to 1 = total loss (Amadio et al., 2019; Dutta et al., 2003; Fuchs et al., 2019b; Gerl et al., 2016; Krzysztofowicz and Davis, 1983; Merz et al., 2013; Smith et al., 1994). This tool is appropriate for the description of damage mechanisms and processes that allow for intermediate states of damage, i.e., between zero and the total loss, like damage to buildings, crops, etc. (these processes are referred to as *progressive* processes in the following). In contrast to vulnerability curves, fragility curves express the relationship between hazard, vulnerability, and the probability of having a certain damage (e.g., Haugen & Kaynia, 2008; McGrath et al., 2019; Nofal et al., 2020; Papathoma-Köhle et al., 2017; Pita et al., 2021; Thapa et al., 2020). Hence, they are profitably used to describe binary processes in which only two states are possible, i.e., "fully safe" (*on-event*) or "fully damaged" (*off-event*), and the damaging occurs very quickly. Hereinafter we define these processes as *on-off* processes, whose typical examples are people or vehicles in floodwater.

Both vulnerability and fragility functions share the use of inundation depth as the main explicative variable for flood damage (Apel et al., 2004; Chen et al., 2019; De Moel et al., 2015; Gerl et al., 2016; Jamali et al., 2018; Hasanzadeh Nafari et al. 2017; Huizinga et al. 2017; Jongman et al., 2012, Kreibich et al., 2009; Lv et al., 2021; Martínez-Gomariz et al., 2021; Zhou et al., 2012). Although it is widely accepted that flood damage is mainly influenced by water depth, this parameter cannot fully explain damage data variance, which, instead, can be explained by a variety of parameters, related both to hazard and to vulnerability (Chen et al., 2016; Dang et al., 2011; Kreibich et al., 2017; McBean et al., 1988; Merz et al., 2004, 2010; Molinari et al., 2014, 2019; Pham et al., 2020; Thieken et al., 2005, 2008), with the latter being strongly dependent on, and varying with, the object under investigation and the physical and socio-economic context in which the flood occurs (Menoni et al., 2012). Nonetheless, vulnerability parameters are often related to socio-economic aspects that can be hardly quantified (Koks et al., 2015), and for which only a qualitative evaluation is possible like the experience of affected people, their level of education, the level of maintenance of a building, etc. (Menoni et al., 2012). This makes the generalization of flood damage assessment tools, as well as their adaptability and transferability in space and time, a challenging task (Cammerer et al., 2013; Molinari et al., 2019, 2020). However, the relationship between damage and hazard variables is more prone to generalization than that with vulnerability's, as it mainly involves physical processes that can be quantified and modelled in mathematical terms. In fact, several studies propose

qualitative fragility curves (e.g., by expressing the probability of damage as low, moderate, and high) as a function of different combinations of water depth and flow velocity, for a variety of objects (see, e.g., Cox et al., 2010; Penning-Rowsell et al., 2005; Ramsbottom et al., 2006).

Limiting the analysis to direct flood damage, this paper presents a general and flexible method to assess the relative damage for *progressive* and *on-off* damage processes using a common framework. The two main ingredients are *i)* a new impact parameter, *W*, which allows to measure flood hazard accounting for both inundation depth and water velocity as flood damage determinants, and *ii)* a procedure to derive the relative damage as a function of *W* quantitatively, starting from physical considerations, empirical, or synthetic damage data. The goal is extending the traditional depth-damage approach accounting for additional explicative variables as flow velocity, yet retaining a relatively simple and intelligible structure.

An explicit, physics-based modelling approach is preferred because physics-based damage models may provide robust results in different contexts and in novel conditions with scarce calibration data, and allow modellers to improve their knowledge and to keep control on the entire process of damage assessment. These aspects are valuable even in the era of big data and complex multi-variate data-based models, whose reliability essentially depends on the quantity and quality of training data (Carisi et al., 2018; Gumiere et al., 2020; Merz et al., 2013; Molinari et al., 2020; Mosavi et al., 2018; Van Ootegem et al., 2015, 2018).

The paper is organized as follows. Section 2 describes the proposed procedure by first introducing the impact parameter *W* (Section 2.1), and then explaining how the parameter can be related to the damage degree or the probability of damage (Section 2.2). Section 3 provides some practical examples on the use of the impact parameter *W* and on the method to derive damage models and fragility functions. Some comparisons with previous approaches are also shown. Finally, Section 4 discusses the work and makes final remarks.

2 An approach for the definition of relative damage functions

Before going into the details of how the impact parameter *W* is defined and can be used, some aspects deserve clarifications. For the sake of simplicity, in the following we use the term "relative damage functions" to denote both vulnerability functions and fragility curves (Cardona, 2004; Cardona et al., 2012; Thywissen, 2006). Indeed, the definition of total damage (for *progressive* damage processes) and of total loss (for *on-off* processes) are very similar to each other:

total damage = relative damage * total value of exposed items

total loss = loss probability * total number of exposed items

The loss probability, as the relative damage, varies between 0 and 1, and increases with the hazard increasing, which supports the general use of "relative damage" in both the cases. Accordingly, relative damage functions can be viewed either in a deterministic sense for *progressive* damage processes, or in a probabilistic sense for *on-off* events.

Depending on the nature of items exposed to floods and on flood features, damage can be ascribed to many diverse processes (e.g., wetting, dragging, drowning), which in turn depend on different explanatory variables, such as water depth and velocity, flood duration, contaminant load, socio-economic status, and precautionary measures (Apel et al., 2009; Bignami et al., 2019; Carisi et al., 2018; Ettinger et al., 2016; Karagiorgos et al., 2016; Kok et al., 2005; Merz et al., 2010; Mignot et al., 2019; Schröter et al., 2014). Accordingly, damage functions are typically highly multidimensional, thus hard to be assessed in a comprehensible and compact form (Papathoma-Köhle et al., 2019). We restrict the analysis to the direct flood damage driven by mechanical processes; in this case, the free variables of relative damage functions reduce to water depth and flow velocity (Balica et al., 2013; Black, 1975; Clausen and Clark, 1990; De Risi et al., 2013; Gallegos et al., 2012; Hammond et al., 2015; Jongman et al., 2012; Martínez-Gomariz et al., 2021; Nadal et al., 2010; Postacchini et al., 2019; Roos, 2003; Zhou et al., 2012). The importance of water velocity in shaping damage has been demonstrated, especially for flash floods, with respect to different damage processes such as physical damage to roads and buildings, stability of people and vehicles, structural damage to buildings (see, e.g., Arrighi et al., 2015; Garrote et al., 2016; Kellermann et al., 2015; Kelman and Spence, 2004; Kreibich et al., 2009; Maiwald and Schwarz, 2015; Martínez-Gomariz et al., 2018; McBean et al., 1988; Milanesi et al., 2018, Postacchini et al., 2021). Therefore, the development of models that include water velocity as an input parameter is expected to reduce flood damage variance with respect to the widely used depth-damage curves (e.g., Pistrika and Jonkman, 2009; De Moel and Aerts, 2011).

2.1 A lumped impact parameter for measuring the flood hazard

We combine the water depth, Y, and flow velocity, U, into a single lumped parameter, named W, so as to express the relative damage as a univariate function, $RD = RD(W)$. The parameter W is then meant to measure the intensity of the hydrodynamic conditions that effectively produces the damage (Aureli et al., 2008). The way in which Y and U combine to form W depends on the kind of exposed items and on the damage process under investigation; therefore, the impact parameter W is expected to assume a form that is object- and process-dependent.

From a deterministic point of view, common parameters that combine flow depth and velocity are flow energy per unit weight, H, and momentum per unit width and weight, M

$$H = Y + \frac{U^2}{2g} = Y\left(1 + \frac{1}{2}F^2\right) \tag{1}$$

$$M = \frac{Y^2}{2} + \frac{U^2 Y}{g} = \frac{Y^2}{2}(1 + 2F^2) \tag{2}$$

where g is gravity and $F = U(gY)^{-1/2}$ the Froude number. Noting the similarity between these two expressions, we propose to use a general impact parameter *W* in the form

$$W = \left(\frac{Y}{Y_W}\right)^{\alpha}(1 + \beta F^2) \qquad \text{with} \qquad Y_W > 0, \;\; \alpha \geq 1, \;\; \beta \geq 0 \tag{3}$$

in which Y_W is a reference depth that scales the actual water depth *Y*, and α and β are two calibration factors that measure the relative importance of the static versus the dynamic component of *W*. Through a proper choice of the two calibration factors, *W* can express the physically relevant concepts of water depth, *Y* (with $\alpha = 1$ and $\beta = 0$), of flow energy, *H* (with $\alpha = 1$ and $\beta = 0.5$), and of momentum, *M* (with $\alpha = 2$ and $\beta = 2$). Thereby, α and β change the nature of *W* among depth, energy, and force (momentum).

The key idea is that, with suitable calibration factors α and β, iso-*W* lines in the *U*-*Y* plane can identify different flow conditions that are equivalent in terms of damaging potential for specific categories of objects and processes; the goal can be achieved as the structure of *W* is able to resemble the physics of the damage process. Advantages of using the impact parameter *W* include: *W* is non-dimensional, it increases monotonically with the damage, and can be arbitrarily scaled through a proper choice of the reference depth, Y_W (for example, *W* can conveniently range from 0 to 1). The use of *W* reduces the dimensionality of the problem and allows for an immediate and intuitive assessment of the hazard degree. In addition, the use of a lumped parameter for identifying the hazard intensity makes the relative damage functions simpler, non-dimensional, and more elegant.

How the calibration parameters α and β affect the meaning of *W* is shown in panels (a)-(c) of Figure 1 where, for $Y_W = 1$ m, three isolines for $W = 0.1$, $W = 0.5$, and $W = 1$, are plotted in the *U*-*Y* plane. Figure 1a ($\beta = 1$) shows that by increasing α the static part of *W* plays a more important role: the isolines reduce their slope and the impact of velocity is lower. Figure 1a shows that iso-*W* lines move upwards with increasing α; as a general rule, $\alpha \approx 1$ makes *W* a good indicator when damage is essentially produced by wetting (i.e., water depth or energy are most involved), whereas $\alpha \approx 2$ is best suited when damage or loss are mainly produced by dragging (i.e., static and dynamic forces are most involved). Figure 1b ($\alpha = 1$) and Figure 1c

(α = 2) show that increasing values of β correspond to an increasing role of flow velocity since iso-W lines become steeper, whereas $\beta \rightarrow 0$ reduces W to a static parameter depending only on the water depth.

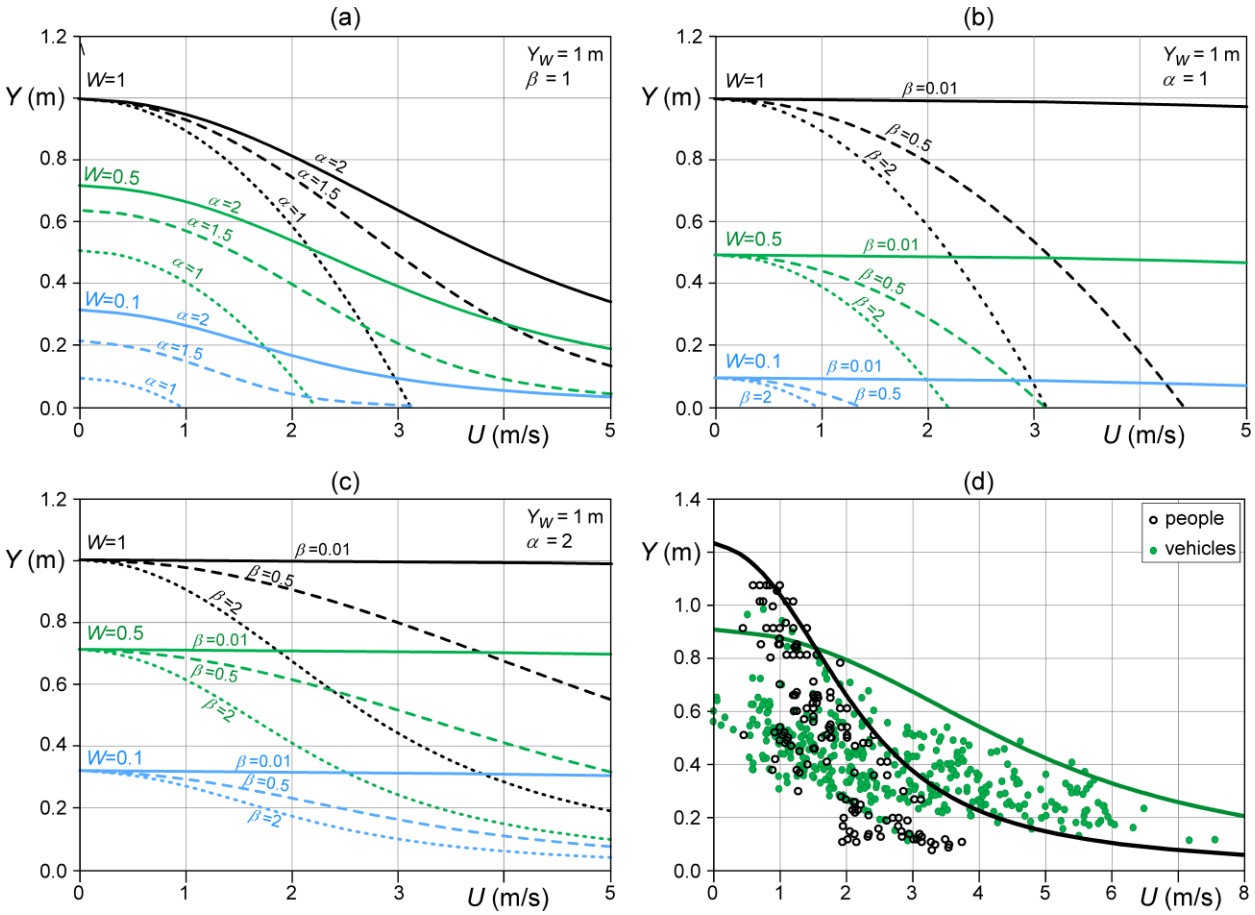

Figure 1. Iso-W lines for different values of the parameter α (a), β with α =1 (b) and β with α =2 (c). (d) Experimental data and W = 1 isolines representing the upper limit for stability of people (black line and dots) and vehicles (green line and dots) exposed to floods (details on data in Sect. 3); the set of parameter for W = 1 isolines are Y_W = 1.25 m, α = 2.0, β = 4.0 for people and Y_W = 0.9 m, α = 2.0, β = 0.6 for vehicles.

The calibration factors of W can be assessed by developing physical models of the damaging process and by analysing critical damaging conditions. A further fine tuning of model parameters might stem from the comparison with available field or lab data.

Here we present a brief overview of the approach; details on the method and data are given in Section 3. Let's consider, for example, the case of people and vehicles exposed to flood flow. Both these categories of objects are subject to dragging, which is a matter of forces. This suggests choosing $\alpha \approx 2$ as for the momentum equation (2) (Kvocka et al., 2016). Physics-based models, as those by Arrighi et al. (2015, 2017) and Milanesi et al. (2015, 2019), provide instability conditions that can be represented by W=1 iso-lines, leading to Y_W = 1.25 m, α = 2.0, β = 4.0 for people and Y_W = 0.9 m, α = 2.0, β = 0.6 for vehicles. Figure 1d

shows, in the *U*-*Y* plane, extreme hazard conditions for people (black dots) and vehicles (green dots) exposed to floods, corresponding to the stability loss. The arrangement of dots clearly shows that limit conditions exist in terms of maximum resistance to flood, for both people and vehicles; these limit conditions correspond to relatively large water depths when the flow velocity is low, and to relatively shallow water depths when the flow velocity is large. In the same Figure 1d, the $W = 1$ isolines described above (black and green lines for people and vehicles, respectively) envelop well the available experimental data, confirming the proper parameterization.

This simple example shows the capability of the impact parameter *W* of describing extreme hazard conditions of items that behave quite differently from one another. The very different values of β needed to fit the experimental data prove the different role played by water depth and flow velocity for people and vehicles quantitatively, providing useful insights for risk management.

2.2 The method to derive relative damage functions

Once the hazard conditions are assessed through the lumped impact parameter *W*, the second point is relating *W* to the damage. In other words, continuous functions providing the relative damage or the probability of *off-events* should be determined for any value of *W*.

The method to construct the relative damage functions is based on the correspondence between iso-*W* and iso-*RD* lines (this correspondence descends from the fact that $RD = RD(W)$ is a univariate function). For *progressive* damage processes, the structure of the impact parameter *W* is determined to make iso-*W* lines matching the shape of iso-*RD* lines; then, a set of couples (*W*, *RD*) is easily found. For *on-off* processes, the tuning of *W* is based on the knowledge of hazard conditions related to *off-events*, which corresponds to $RD = 1$ conditions; the relative damage is then given by the cumulative frequency distributions (CFD) of *W* associated to the *off-events*. Finally, (*W*, *RD*) couples or discrete CFDs can be suitably approximated to provide the relative damage functions.

3 Applications

In the present section, the lumped impact parameter *W* and the procedure to construct the relative damage functions are applied to three cases of practical interest. Given that the definition of relative damage and its assessment slightly differ when considering *on-off* or *progressive* damage processes, we analyse the stability of people and vehicles for the first type of process, and the damaging of buildings for the second one. These applications are only aimed at describing the use of the impact parameter *W* and the method to assess relative damage functions, showing both the advantages and the limitations of the proposed approach.

3.1 Stability of people in floodwaters

3.1.1 Impact parameter W

Vulnerability of people due to stability loss in flowing water can be seen as an *on-off* process. The resistance of people to flowing water depends on different aspects such as age, sex, weight, height, experience (Lind et al. 2004). This suggests that different relative damage functions can be defined according to the sub-categories of people considered. However, as long as the impact parameter W is able to capture the physical mechanisms of damage, which is the same for any individual, a unique structure of W, given by a set (Y_W, α, β), can be defined for the whole population (see Appendix A). Relative damage functions for sub-categories can then be defined by considering different values for the impact parameter. Here, for simplicity, we consider only two broad sub-categories, namely adults and children.

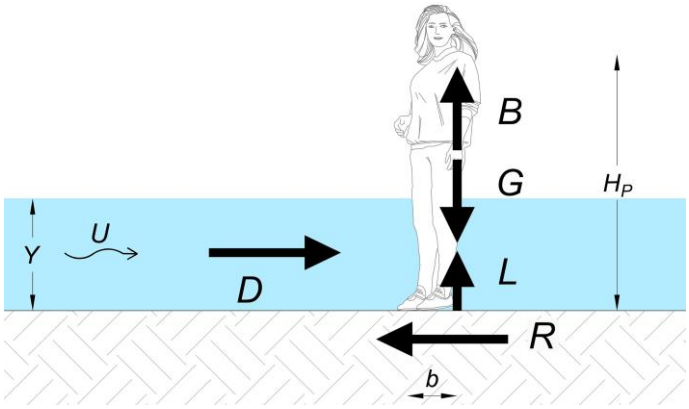

Figure 2. Schematics of forces acting on a human body exposed to floodwaters.

Assuming the loss of balance as full damage condition, the calibration factors of W are estimated starting from a physical point of view considering the stability of a human body in floodwaters. Referring to a simple instability model (Figure 2), the forces acting on a human body are (Milanesi et al., 2015; Wang and Marsooli, 2021; Xia et al., 2014a):

$$\begin{aligned} &\text{Drag} && D = \tfrac{1}{2}\rho C_D w Y U^2 \\ &\text{Lift} && L = \tfrac{1}{2}\rho C_L w Y U^2 \\ &\text{Weight} && G = \rho_P g (H_P w b) \\ &\text{Buoyancy} && B = \rho g (Y w b) \end{aligned} \tag{4}$$

where ρ and ρ_P are the water and body densities, C_D and C_L are the drag and lift coefficients, H_p the body height measured at shoulders, w the frontal body width, and b the average length of the body in the flow direction.

Instability may occur by toppling or sliding mechanisms, depending on the Froude number (Arrighi et al., 2017). Here we focus on sliding instability, typical of lower depths and higher flow velocities, but similar reasoning applies to toppling mechanism. The critical stability condition for sliding is

$$D = (G - B - L)\mu \tag{5}$$

where μ is the friction coefficient. Using Eqs. (4) and solving Eq. (5) for the squared velocity, we obtain

$$U^2 = \frac{2gb\mu}{C_D + \mu C_L}\left(\frac{H_P}{Y} - 1\right) \tag{6}$$

The $W = 1$ isoline for people is easily obtained from Eq. (3) to read

$$U^2 = \frac{gY}{\beta}\left[\left(\frac{Y_W}{Y}\right)^{\alpha} - 1\right] \tag{7}$$

Comparing Eqs. (6) and (7), we find $\alpha = 2$ and $Y_W = H_p$; in fact, with these parameters, Eq. (7) can be rewritten as

$$U^2 = \frac{gY}{\beta}\left[\left(\frac{H_P}{Y}\right)^2 - 1\right] = \frac{gY}{\beta}\left(\frac{H_p}{Y} + 1\right)\left(\frac{H_p}{Y} - 1\right) = \frac{g\left(H_p + Y\right)}{\beta}\left(\frac{H_p}{Y} - 1\right) \tag{8}$$

Combining Eqs. (6) and (8) to eliminate U^2, we find

$$\beta = \frac{C_D + \mu C_L}{2\mu}\left(\frac{H_P + Y}{b}\right) \tag{9}$$

The parameter β, which multiplies the Froude number in Eq. (3), controls the relative importance of the dynamic component of W; it plays a role when the Froude number is relatively high, and becomes irrelevant in the limit $F \to 0$. Accordingly, a significant estimate of β can be obtained in the limit $F \to \infty$, which corresponds to $Y \to 0$. In this case, Eq. (9) provides

$$\beta = \frac{C_D + \mu C_L}{2b\mu} H_P \tag{10}$$

Considering a drag coefficient, C_D, in the range 1.0–1.2, a lift coefficient $C_L \approx 0$, a friction coefficient μ in the range 0.3–0.5, and the lengths b = 0.25–0.35 m and H_p = 1.20–1.50 m, the calibration factor β varies in the range 3.0–7.0 for adults.

Then, the best values of Y_W and β can be found based on available experimental data. Indeed, many theoretical and experimental studies are available in the technical literature concerning the stability of people exposed to flood waters. The variety of data obtained from different experiments does not represent real flooding conditions, yet it allows for a robust evaluation of the limiting condition for the stability of people exposed to floodwaters. Figure 3 collects data from the studies by Foster and Cox (1973), Abt et al. (1989), Takahashi et al. (1992), Karvonen et al. (2000), Yee (2003), Jonkman and Penning-Roswell (2008), Russo et al. (2013), Xia et al. (2014a), Milanesi et al. (2015), Chanson and Brown (2015, 2018), Martínez-Gomariz et al. (2016), Milanesi et al. (2016), and Arrighi et al. (2017). Such data can be considered sufficiently homogeneous and representative of different sub-categories of individuals at the same time, as they all refer to loss of stability in a variety of physical and boundary conditions and at the first attempt, i.e., when the person exposed to the flow does not have any experience. The latter condition is the reason why the dataset from Abt et al. (1989), although reported in the figure, is not accounted for in assessing the curves; in fact, the purpose of the experiments performed by Abt et al. (1989) was to identify the absolute limit of stability of people that, being tested several times in similar conditions, learned how to cope with floodwaters.

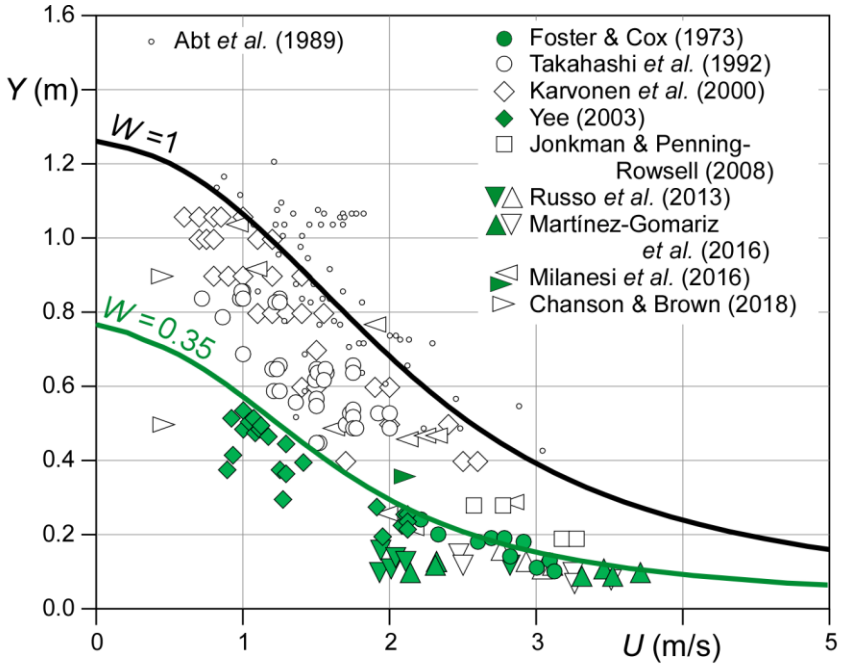

Figure 3. Experimental data and iso-W lines for instability of adults (black line and open symbols) and children (green line and symbols).

We choose the isoline $W = 1$ to represent the upper limit of the *off-events* detected in all the experimental data of Figure 3 (i.e., $W_{LIM} = 1$ identifies the critical condition for the most resistant items in

the whole category). By adjusting the model parameters, we find Y_W = 1.25 m, α = 2.0, and β = 4.0, which corresponds to the black iso-W line in Figure 3. It is worth observing that, with these values of α and β, the impact parameter W identifies momentum as the main damage determinant, in line with the underlying physical processes (i.e., dragging).

The upper limit in Figure 3, as well as the values chosen for (Y_W, α, β), are dictated by the resistance of the adult sub-category. As previously noted, the vulnerability of sub-categories should be characterized by lower values of the impact parameter, yet with the same parameter structure, i.e., by keeping Y_W, α, and β fixed. The critical threshold W_k^{LIM} for the k-th sub category is then a fraction of the critical impact parameter of the reference (most resistant) sub-category, W_{LIM}, according to

$$\frac{W_k^{LIM}}{W_{LIM}} = \left(\frac{Y_{W_k}}{Y_W}\right)^{\alpha} \tag{11}$$

The above relation (see Appendix A) means that the critical value for the k-th sub-category, W_k^{LIM}, depends only on the physical parameters describing the k-th sub-category (i.e., on Y_{Wk}), and it is independent of hydrodynamics. Figure 3 shows that the limit condition for children (younger than 18 years old) is well described by the $W = W_k^{LIM} = 0.35$ isoline (green line).

3.1.2 Relative damage functions

The second step consists in assessing the relative damage functions, according to the method outlined in Sect. 2.2. A sufficiently large and representative sample of *off*-conditions should be considered. For the case of people stability, a rich experimental dataset is available (Figure 3). From each pair (U_i, Y_i) of the *off-events*, the associated value of W_i is computed using Eq. (3). The cumulative frequency distribution of W_i for the two sub-categories, plotted in Figure 4a, gives the relative damage curve, i.e., the probability to fail, for each single individual belonging to a given sub-category.

It is often convenient to interpolate the discrete cumulative distributions inferred from the data with a continuous function to express the relative damage. Among the possible forms, a simple and effective expression is

$$RD(W) = \frac{1}{1 + (a/W)^b} \tag{12}$$

Figure 4a compares the relative damage functions obtained for the two sub-categories; note that this is possible only because the hydrodynamic hazard is described by the same impact parameter. For the case of

people, a good fit of the discrete data is found using Eq. (12) with a = 0.25 and b = 6 for children (green line in Figure 4) and a = 0.6 and b = 5.0 for adults (black line in Figure 4).

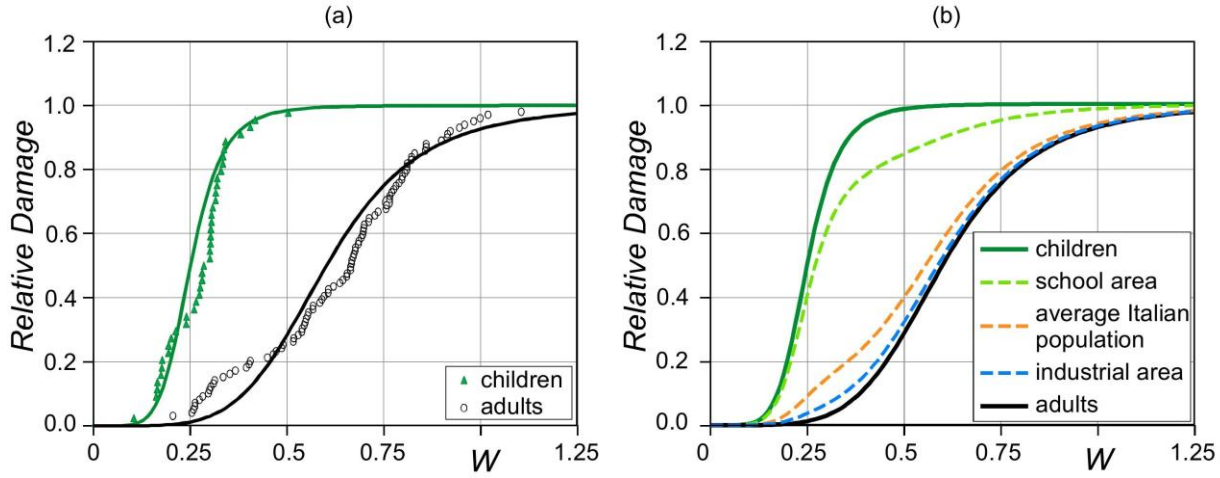

Figure 4. a) Cumulative frequency distributions of *off-events* for children (green) and adults (black) based on data of Figure 3, approximated with Eq. (12) to provide the relative damage functions. b) Examples of relative damage functions for different age distribution of people.

Thanks to the use of a single impact parameter to describe the hydrodynamic hazard for different sub-categories, the corresponding relative damage functions can be combined to provide a unique function for the whole category, as a weighted average of the sub-category relative damage functions:

$$RD(W) = \sum_{j=1}^{N} \varphi_j RD_j(W) \tag{13}$$

where N is the number of sub-categories, φ_j is the percentage of objects belonging to the j-th sub-category, and $RD_j(W)$ is the associated relative damage curve.

For example, one can easily derive the relative damage functions for population living in countries with different distribution of children and adults (e.g., the proportion of children is larger in Asian than in European countries), or for people that typically frequent different districts of a city (e.g., the fraction of children is different in industrial and school areas, making school areas more vulnerable). An example is shown in Figure 4b where, starting from the relative damage functions for adults and children (green and black lines), we compute the relative damage functions for the Italian population (orange line) considering 16% of children and 84% of adults according to ISTAT (2020), for an industrial area assuming 5% of children and 95% of adults (blue line), and for a school area assuming 80% of children and 20% of adults (light green line).

3.1.3 Comparison with previous approaches

Comparing the proposed approach with previous ones provides some interesting insights. Indeed, some formulations have been previously proposed both in the scientific literature and in flood-risk manuals to express flood damage for people in terms of a single hazard parameter, which combines flow depth and velocity (e.g., AIDR, 2017; BWW, BRP, BUWAL, 2008; Cox et al., 2010; De Moel et al., 2009; Ramsbottom et al., 2006; Smith et al., 2014). In these works, damage is classified with the use of thresholds that provide qualitative descriptions of vulnerability rather than quantitative measure of the expected damage. Unfortunately, the use of dimensional parameters and of thresholds that are based on empirical evidence, led to damage definitions lacking a clear meaning or with a weak physical constitution; the significant discrepancies among the degree of damage predicted by different formulations, as detailed in the following, are signs of these weaknesses.

For example, Ramsbottom et al. (2006) introduced the Hazard Rating index $HR = Y\,(U+0.5)$ and defined four ranges of HR corresponding to four qualitative probabilities of damage: *low* ($HR < 0.75$), *moderate* ($0.75 < HR < 1.25$), *significant* ($1.25 < HR < 2.5$), and *extreme* ($HR \geq 2.5$). Cox et al. (2010) used the Product Number $PN = U \cdot Y$ to identify the same four classes of damage probability (thresholds for PN are 0.6, 0.8, and 1.2 m²/s), with additional conditions entailing the *extreme* damage probability when either $U > 3.0$ m/s (for both adults and children), $Y > 1.2$ m (for adults), or $Y > 0.5$ m (for children).

In order to compare the two above classifications, we compute the values of HR and PN for pairs (U, Y) in the range $0 \leq U \leq 5$ m/s and $0 \leq Y \leq 2.5$ m and check for the agreement between the associated risk classes. The results are reported in Figure 5a for adults and in Figure 5b children: shaded areas denote the domain of all possible PN and HR; the grey and the coloured areas mark agreement and disagreement between the two approaches, respectively. Consider two examples of the damage probability for adults: the couple (U =3 m/s, Y = 0.2 m) leads to HR = 0.7 and to PN = 0.6, both corresponding to the *low* class (the two criteria agree, this point falls in the grey area of Figure 5a); on the other hand, the couple (U = 3.1 m/s, Y = 0.2 m) leads to HR = 0.74 (*low*) and to PN = 0.64 (*extreme* because of $U > 3$ m/s), i.e., the probability of damage is three classes higher using PN rather than HR (this point falls in the dark red area in Figure 5a).

For the children sub-category, the classes of damage are three (*moderate* and *significant* are merged). By looking at Figure 5b, for children there are hazard conditions corresponding to *moderate/significant* damage using HR and to *extreme* using PN (large yellow area), and even worse, *low* damage probability using HR and *extreme* using PN (orange area). A partial reason for the above differences could be found in the use of the Abt et al. (1989) dataset to determine the HR thresholds (Ramsbottom et al., 2006). The lack of a proper physical base of the above criteria likely played a role as well.

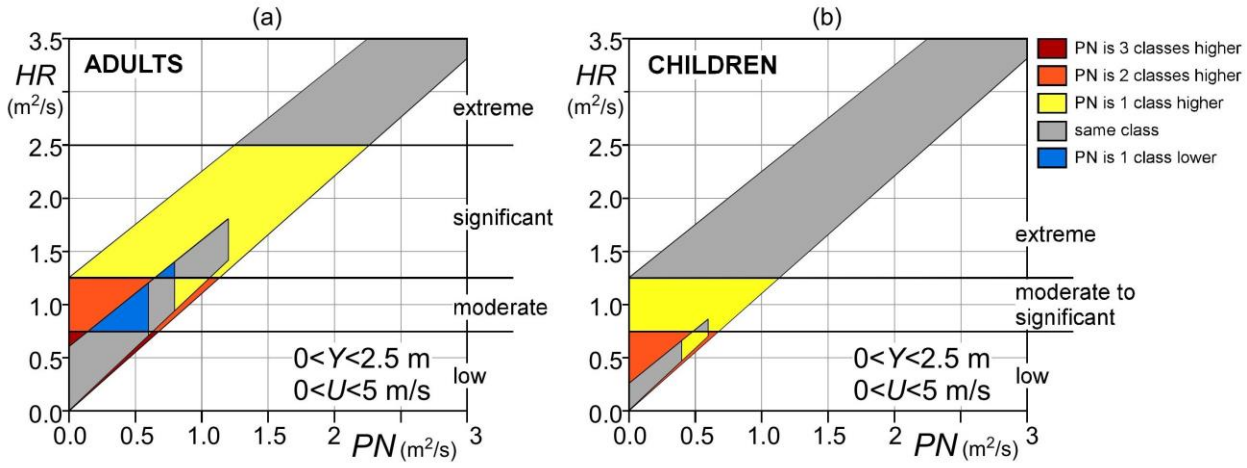

Figure 5. Comparison between two approaches of damage probability assessment for adults (a) and children (b) exposed to floods: the *HR* index by Ramsbottom et al. (2006) and the *PN* index by Cox et al. (2010); grey areas identify either mutual agreement, coloured areas different degree of disagreements.

A comparison of the impact parameter *W* with the *HR* and *PN* criteria for assessing damage probability of adults (black lines and symbols) and children (green lines and symbols) is shown in Figure 6; the isolines corresponding to extreme conditions according to the different criteria are superposed to the experimental data. As observed, the iso-*HR* lines tend to overestimate the actual stability conditions whereas the iso-*PN* lines fit the experimental data very well for flow velocities between 1 and 3 m/s. Yet, for the lowest and highest velocities, the iso-*HR* and iso-*PN* lines are not physically sound; for example, when $U = 0$ m/s, the *HR* approach predicts extreme conditions only for a water depth greater than 5 m, which is a very large value in real flooding events (indeed, for the case $U = 0$, the *extreme* limit *HR*=2.5 corresponds to $Y = 5$ m; Kvocka et al., 2016).

The *PN* approach excludes unrealistic results thanks to additional thresholds (horizontal and vertical dashed segments in Figure 6b). Nonetheless, the upper limit of $U = 3$ m/s seems too much clear-cut, since some experimental data lay well beyond.

Interestingly, the iso-*W* lines, with suitable calibration factors, well envelope the available experimental data and are consistent with the common sense as well.

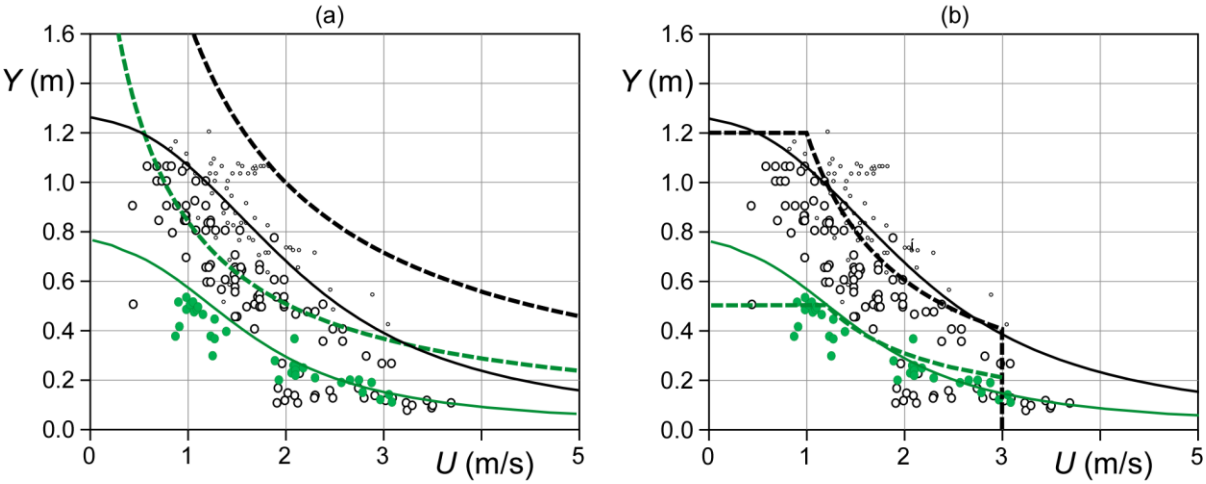

Figure 6. Stability conditions of adults (black) and children (green): experimental data (dots) and hazard threshold corresponding to extreme damage probability according to iso-*W* (solid lines), iso-*HR* (dashed lines in panel a) and iso-*PN* lines (dashed lines in panel b).

3.2 Stability of vehicles in floodwaters

A second application of the method to *on-off* damaging processes, involving vehicles, is shortly presented. As for the case of people, instability of vehicles in floodwaters occurs due to a sliding mechanism caused by drag. The physical problem is slightly complicated for the presence of the gap between the car and the ground (Martínez-Gomariz et al., 2018; Milanesi and Pilotti, 2019; Xia et al., 2011) and uncertainty about watertightness of vehicles (Bocanegra et al., 2020). Many studies in the technical literature relate the *on-off* damaging condition of vehicles in flowing water to the (in)stability condition of the vehicle (Figure 7 collects data from Bonham and Hattersley, 1967; Gordon and Stone, 1973; Keller and Mitsch, 1993; Kramer et al., 2016; Martínez-Gomariz et al., 2018; Martínez-Gomariz et al., 2019; Milanesi and Pilotti, 2019; Oshikawa et al., 2011; Shand et al., 2011; Shu et al., 2011; Smith et al., 2019; Teo et al., 2012; Toda ed al., 2013; Xia et al., 2011; Xia et al., 2014b). Within the vehicle category, we consider three different sub-categories: small-to-medium cars, medium-to-large cars, SUVs and VANs. The last category is taken as reference since it is the most resistant.

Here, to determine the calibration factors of *W*, it is more convenient to adopt a data-driven procedure, which considers the physics of the problem as well. Since the instability is drag driven, a reasonable choice for the parameter α is 2, so that the static contribution to *W* corresponds to the hydrostatic force. To fit the upper limit of stability of available data with a $W = 1$ iso-line, suitable values of the model parameters are $Y_W = 0.9$ m and $\beta = 0.6$. These values correspond to the most resistant VANs and SUVs.

The limit stability conditions for the weaker sub-categories are well described using the same values of Y_W, α, and β, by isolines characterized by lower values of W; specifically, $W = 0.50$ for medium-to-large and $W = 0.35$ for small-to-medium vehicles (Figure 7). The fact that the same structure of the impact parameter W allows to describing the limit conditions of different sub-categories confirms that the physics-based and flexible structure of W well captures the key aspects of the damaging process of items within a given category.

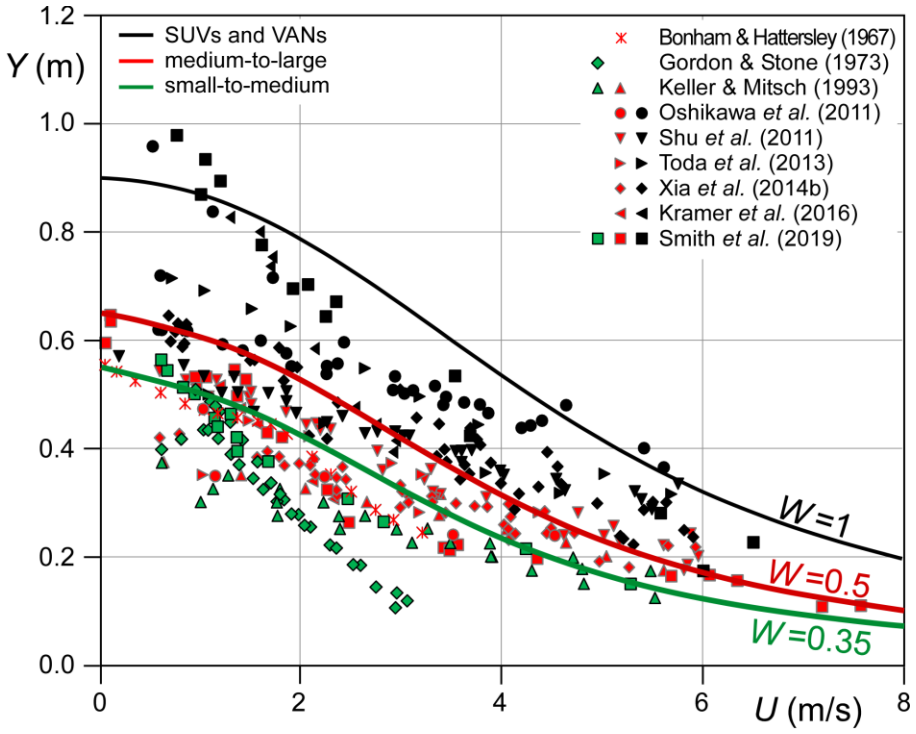

Figure 7. Experimental data and iso-W lines for instability of small-to-medium vehicles (green line and symbols), medium-to-large vehicles (red line and symbols), SUVs and VANs (black line and symbols).

The cumulative frequency distributions for each sub-category (Figure 8) are evaluated using the data of Figure 7, and are interpolated with continuous relative damage functions using Eq. (12).

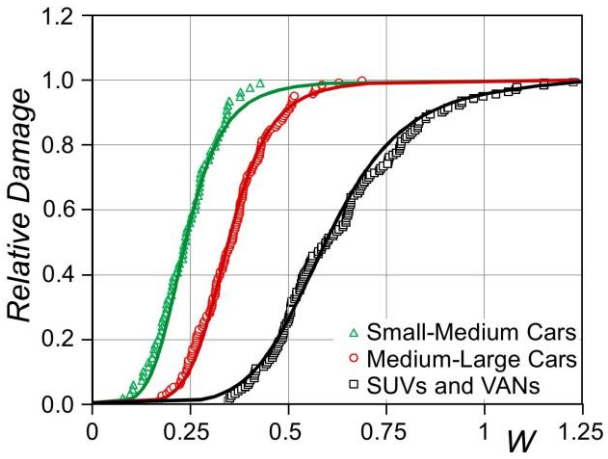

Figure 8. Cumulative frequency distributions for vehicle sub-categories and associated relative damage functions by fitting Eq. (12) for small-to-medium cars (green, a = 0.60 and b = 6.0), medium-to-large cars (red, a = 0.35 and b = 6.5), SUVs and VANs (black, a = 0.24 and b = 5.2).

3.3 Damage of buildings

The procedure for assessing the vulnerability of objects subject to *progressive* damage is slightly different from that of *on-off* damage processes. To show this, we use damage to residential buildings as an example. Experimental data on damage to buildings are scarce in the literature, often refer to *on-off* damage processes (i.e., the collapse of buildings) and are unsuitable for the objective of the analysis, as they usually express damage in absolute terms, rarely report information about flood velocity, and do not contain enough information on building characteristics, hampering their classification in classes of similar "resistance". For these reasons, we base our analysis on relative damage data (*RD*) provided by the synthetic damage model INSYDE (Dottori et al., 2016; Molinari & Scorzini, 2017). INSYDE is a synthetic probabilistic flood damage model based on a component-by-component explicit cost analysis, and it is especially appropriate for our aim, as it considers the role of many hazard variables in shaping damage (including water depth and flow velocity), as well as the main characteristics of buildings that determine their propensity to be damaged in similar ways.

Here, we consider residential buildings with standard Italian features and geometry; the variables "building structure" and "number of floors" are allowed to vary, forming four sub-categories of buildings (i.e., reinforced concrete or masonry buildings, with 1 or 2 floors). The flood duration is assumed constant, i.e., 6 h, whereas sediment and contaminant loads are neglected in order to evaluate only the dependence of damage on water depth and velocity. In detail, for each sub-category, the INSYDE model is forced with a set of (U, Y) input data to generate a set of (U, Y, RD).

The first step for the definition of the damage model is determining the structure of the impact parameter W, i.e., finding suitable values of Y_W, α, and β. Recalling the link between iso-W and iso-RD lines in the (U, Y) plane (Sect. 2.2), the set of (U, Y, RD) triplets provided by the INSYDE model allows identifying iso-RD lines in the (U, Y) plane, which makes the procedure more robust than for *on-off* damage processes. Since RD = 100% points in the (U, Y) plane are generally not available for objects subject to *progressive* damage (total damage entails extreme, thus rare, forcing conditions), matching the RD = 1 limit condition with W = 1 isolines makes little to no sense. A sensible choice must be done to define, for each sub-category, the value of RD associated to W = 1. This value becomes a sort of reference relative damage and, differently from the case of *on-off* data, values of $W > 1$ can be expected for high hazard conditions. We then set Y_W equal to the physically meaningful threshold Y_W = 3.5 m, which corresponds to the typical height of the first floor in Italy. Of course, choosing Y_W equal to the first-floor height is just one of the possible choices.

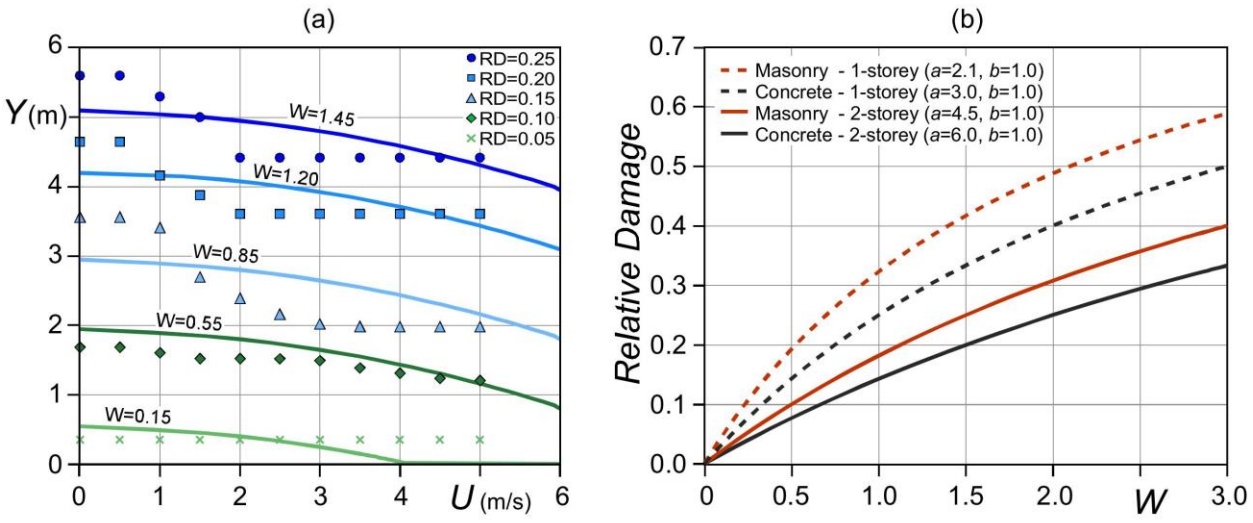

Figure 9. a) RD = const. point data obtained for two-storey masonry buildings as provided by the INSYDE model, then interpolated with iso-W lines with α = 1 and β = 0.3. b) Relative damage functions for the four building sub-categories: single-storey (dashed lines) and two-storey (solid lines), concrete (grey) and masonry (red) buildings.

Proper values of the α and β factors can then be found by making the shape of iso-W and iso-RD lines as similar to each other as possible. In doing so, the analysis of the damage mechanisms can be of further support. For the case under investigation, physical reasoning suggests choosing α = 1, as damage to buildings is mainly due to wetting, which depends on water depth (and flow energy) rather than on flow force (Gems et al., 2016). Moreover, for $U \approx 0$, the impact parameter W reduces to a non-dimensional measure of the water depth Y (scaled with the first-floor height). The best fit of data provided by INSYDE

then leads to a suitable value of β. Figure 9a displays the results obtained for the case of two-storey masonry buildings. For this sub-category, we obtain $\beta = 0.3$, a relatively low value that confirms the marginal role of flow velocity and locates the structure of W between water depth and specific energy (Leelawat et al. 2014; Kreibich et al., 2009; Scorzini et al. 2017). Looking at Figure 9a, where the different symbols represent RD = const. conditions, the dependence of RD on the flow velocity, U, seems not well captured by iso-W lines. The reasons are manifold: the flow velocity naturally plays a minor role in building damaging than for items subject to instability; furthermore, the INSYDE model contains simplifications and idealizations that include the linearization of processes and the use of internal thresholds (e.g., the value of U becomes irrelevant from 2-3 to 5 m/s).

Associating iso-W and iso-RD lines provides couples of (RD, W) for each sub-category; the interpolation of these points with a monotonically increasing relationship, such as Eq. (12), gives the relative damage function (Figure 9b). As for the previous cases, the relative damage functions for different kinds of buildings can be compared on the same plot; this is because hazard conditions are described by a structure of the impact parameter W that is shared by all the sub-categories here considered.

In order to verify the effectiveness and accuracy of the proposed procedure based on the impact parameter W, we generate random values for (U, Y) pairs with $0 < U < 5$ m/s and $0 < Y < 5$ m. We then compute the corresponding values of relative damage using the INSYDE model and compare the results with the corresponding relative damage values provided by the relative damage functions of Figure 9b for the two-storey masonry building sub-category. The comparison, reported in Figure 10, shows a good agreement, with a correlation coefficient $R^2 = 0.95$.

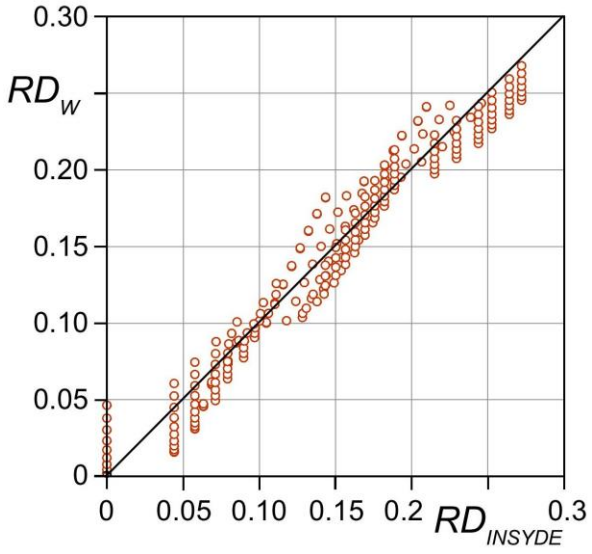

Figure 10. The relative damage predicted by the INSYDE model, RD_{INSYDE}, versus the one computed with the proposed procedure based on the impact parameter W, RD_W.

4 Discussion

The idea of combining the water depth and velocity to express flood hazard is not new. Functional relations involving flow depth and velocity (or, equivalently, the Froude number) are the typical outcome of physics-based studies for flood loss of people and vehicles (e.g., Arrighi et al.,2015, 2017; Jonkman and Penning-Roswell, 2008; Lind et al., 2004; Martínez-Gomariz et al., 2016, 2019; Milanesi and Pilotti, 2019; Milanesi et al., 2015; Postacchini et al., 2021; Shu et al., 2011; Smith et al., 2019; Xia et al.,2014a, 2014b). Aureli et al. (2008) introduced the *total depth* $D = Y\sqrt{1 + 2F^2}$, which includes the effect of flow inertia and represents the water depth at rest whose static force is equivalent to the total force of the flow. Combined with the outcomes of hydrodynamic models (Ferrari et al., 2019, 2020), the *total depth* provides a spatially distributed picture of the hazard degree that is particularly significant for items subject to dragging (i.e., when loss is a matter of forces). Kreibich et al. (2009) explored the dependence of flood damage on different parameters involving flow depth and velocity, concluding that the choice of the "best" parameter(s) depends on the kind of items considered. Among these parameters, the product of flow depth and velocity, $Y{\cdot}U$, known as *flow intensity* (Kreibich et al., 2009), *Product Number* (Cox et al., 2010), or *flow magnitude* (Arrighi et al., 2020), found widespread applications in the loss assessment of people and vehicle in floodwaters (e.g., AIDR, 2017; Costabile et al., 2020). A quite similar index is the *Hazard Rating*, $HR = Y\,(U+0.5)$, introduced by Ramsbottom et al. (2006) and commented in previous Section 3.1.3. As an important aspect, many of the above impact parameters need to be complemented by specific thresholds which apply to basic quantities. A notable example is the $Y{\cdot}U$ product number, which does not represent any physically relevant principle and requires thresholds on both water depth and velocity to provide a measure of the risk degree in general conditions (AIDR, 2017; Cox et al., 2010).

The multifaceted picture of functional relations and impact parameters cited above suggests: *i) need for specific impact parameters* to capture the damage processes of different kind of exposed items; *ii) the fragmentation of approaches, methods and outcomes* deriving from a wealth of valuable studies dealing with specific object categories, with a lack of common vision; *iii) some inconsistencies* that are the unavoidable consequence of fragmentation or insufficient physical foundation (of which the extensive use of thresholds is a symptom). These three factors act to limit the general applicability of previous methods and, in some cases, their robustness as well. While the first one is intrinsic of the problem, the last ones deserve further attention. The method we propose is a step to overcome these drawbacks, as:

- the impact parameter W is non-dimensional, thus expressing a degree of hazard independent of specific dimensions. If opportunely scaled, it provides an immediate measure of the hazard degree, also when hazard is determined by particular combinations of both water depth and flow velocity. This allows for an enhanced comprehension of damage causes and processes;

- the impact parameter *W* is flexible, hence capable of representing various damage mechanisms within a common frame. As shown in the above applications, this allows encompassing and complementing previous works on flood vulnerability, which included water depth and velocity as explanatory variables. Indeed, previous studies and analysis can be recast in a general, common framework that allows obtaining elegant, single-variable relative damage curves for item categories subject to either *progressive* or *on-off* damage;
- the impact parameter *W* has a physical foundation, as it ranges between the concept of energy and momentum, and it can be fitted to available experimental and field data effectively without the need of additional thresholds. This is expected to enhance the robustness of damage predictions, also with respect to high-dimensional multi-variate models that can be ill-conditioned in case of scarce data (Carisi et al., 2018; Merz et al., 2013; Wang et al., 2015).

The applications shown in Section 3 proved that a given structure of the *W* parameter (i.e., a couple of parameters α and β) allows capturing the mechanisms of damage for categories of objects that share the same nature (e.g., people, vehicles, etc.) and are exposed to the same damage process. Thus, a single structure of *W* can be used to express the hazard degree of different sub-categories that group objects characterized by different resistance. This allows comparing the vulnerability of different items belonging to the same category, and to express the vulnerability of a category depending on its composition by weight-averaging the relative damage functions of sub-categories. This is particularly useful for comparing different vulnerability contexts and facilitates the evaluation of absolute (or total) damage when exposure is uniform within the different sub-categories. In other words, the use of *W* allows expressing the hazard degree as a function of a single parameter, thus enhancing the intelligibility of hazard information and simplifying damage assessment.

Another remark regards the vulnerability of buildings. We applied the proposed procedure considering the progressive damage caused by wetting, which is the most challenging application because of the structure of the impact parameter *W* and of the marginal role played by flow velocity. This choice was aimed at testing the flexibility of *W*. Better results are expected from the application of *W* to the case of building stability, which can be undermined as a result of flow drag and buoyancy (Black, 1975; Mazzorana et al., 2014). The physics of the problem shares fundamental similarities with the loss of stability of people and vehicles in floodwaters. Indeed, the shape of stability thresholds for buildings (Dale et al., 2004; Middelmann-Fernandes, 2010; Bignami et al., 2019), is very similar to the *W*-isolines obtained in Sect. 3.1 and 3.2.

A common aspect that can be observed in many studies on flood risk for *on-off* items is the lack of fragility curves describing the actually gradual variation of the loss probability with the hazard degree. In

some cases, the assessment is limited to hazard degree thresholds (e.g., Middelmann-Fernandes, 2010); often, the probability of loss is expressed by means of classes (e.g., Cox et al., 2010; Kvocka et al., 2016, Ramsbottom et al., 2006), which makes difficult to obtain quantitative results (e.g., expected losses). Moreover, the identification of these classes is based on empirical considerations. In other cases, flood hazard rating is assumed to vary linearly with the ratio of the actual flow velocity to the incipient velocity, i.e., the velocity at which person loses stability in floodwater (Kvocka et al., 2016), but the real correspondence between hazard rating and fragility remains unknown. The method we proposed to derive fragility curves (Section 2.2) allows expressing the loss probability explicitly. It is based on the knowledge of a set of loss conditions, derived either from experimental/field data, or from physics-based models forced with a representative set of input data (e.g., for varying the characteristics of exposed items).

A future development regards the inclusion of other variables within the impact parameter. An example is the wind velocity, that can contribute to human's vulnerability as demonstrated in the recent study on storm-induced coastal flooding by Wang and Marsooli (2021). Another important aspect that needs to be considered is the forcing duration, which in fact deserves a particular attention; damaging develops in time, and the rate at which damage develops depends on the time variation of the forcing factors. On one hand, hydrodynamic models able to provide a spatially explicit, detailed, and accurate temporal evolution of water depth and flow velocity in flooded areas at local and regional scales are now largely available (e.g., Ferrari et al., 2019; Ferrari & Viero, 2020; Lacasta et al., 2014; Sanders & Schubert, 2019); on the other hand, expressing the hazard degree with a single impact parameter is beneficial to describe time-dependence of the damage.

5 Conclusions

In the present study, a procedure is outlined to assess flood relative damage functions based on one single impact parameter describing the hydrodynamic action. The proposed impact parameter, W, has a physics-based, flexible form that allows estimating the flood hazard degree for items subject to diverse damaging processes. It is particularly useful when both water depth and flow velocity play a role in the damage process. The application of the proposed impact parameter to assess the vulnerability to floods of people, vehicles, and residential buildings, confirmed the flexibility of the formulation and showed advantages of using a physics-based, explicit approach.

Relative damage functions are assessed through a data-driven procedure, which is based on the use of either real data (both synthetic or experimental) bearing sufficient information on flood features (i.e., hazard degree) and the damage to exposed items. After determining a suitable structure of the impact parameter W, the relative damage functions are assessed in a probabilistic framework for *on-off* damage process like

those related to the stability of people or vehicles in flowing water, and with a deterministic fitting procedure for *progressive* damage processes. Yet, the relative damage functions obtained through the two approaches are equivalent for practical application purposes.

Adopting the impact parameter W, traditional depth-damage functions and fragility curves are enhanced by including the flow velocity as hazard determinant, and multi-variable damage functions are reverted to simpler and more elegant single-variable, non-dimensional functions. Previous damage and loss models can be recast in a unique, simple, and elegant form. The flexibility of the present formulation also allows for an easy merging of physics-based reasoning and available data, which can result in enhanced model robustness.

Appendix A. Impact parameters for different sub-categories

Here we derive, in terms of impact parameter W, the limit condition of full loss for different sub-categories of exposed items. Without loss of generality, let us consider two sub-categories and start looking at each sub-category as a single category. For the most resistant category, denoted as *reference category*, eq. (3) defines the impact parameter for given Y_W, α, and β:

$$W = \left(\frac{Y}{Y_W}\right)^{\alpha} (1 + \beta F^2) \tag{14}$$

The full loss of items in the reference category is denoted by the limit condition $W = W_{LIM}$ (for simplicity, this limit can be thought as $W_{LIM} = 1$). For the k-th weaker sub-category, taken individually, the impact parameter is

$$W'_k = \left(\frac{Y}{Y_{W_k}}\right)^{\alpha} (1 + \beta F^2) = \left(\frac{Y_W}{Y_{W_k}}\right)^{\alpha} \left(\frac{Y}{Y_W}\right)^{\alpha} (1 + \beta F^2) = \left(\frac{Y_W}{Y_{W_k}}\right)^{\alpha} W \tag{15}$$

In Eq. (15), the parameters α and β remain the same as in Eq. (14), as the physics of damage process is the same for the whole category. Again, Y_{Wk} is chosen to identify the sub-category limit condition of full loss as $W'_k = W_{LIM}$. In this way, for a given flow condition (Y, F), the resulting impact parameter is different for each sub-category; in particular, larger values are obtained for weaker sub-categories (i.e., $W'_k > W$), since Y_{Wk} is smaller than Y_W. This occurrence is indeed annoying; for example, it prevents plotting iso-W lines of different sub-categories onto the same (Y-U) plane.

It is far more convenient to have a biunivocal correspondence between W and the flow conditions (Y, F) for an entire category of similar exposed items. This is achieved by rescaling the impact parameter of

weaker sub-categories, W'_k, by a factor $(Y_{Wk}/Y_W)^{\alpha}$, which corresponds to using a single reference depth, namely Y_W, for the whole category. The limit condition associated to the k-th sub-category, denoted with W_k^{LIM}, is rescaled accordingly:

$$W_k^{LIM} = \left(\frac{Y_{W_k}}{Y_W}\right)^{\alpha} W_{LIM} \tag{16}$$

As a final result, for a given flow condition (Y, F), the impact parameter W is the same for different sub-categories. For items belonging to the k-th sub-category, the hazard degree is then expressed by the ratio W/W_k^{LIM}.

CRediT authorship contribution statement

Tommaso Lazzarin: Conceptualization, Methodology, Investigation, Visualization, Writing - Original Draft **Daniele Pietro Viero:** Methodology, Visualization, Writing - Review & Editing **Daniela Molinari:** Methodology, Writing - Review & Editing **Francesco Ballio:** Methodology, Writing - Review & editing. **Andrea Defina:** Conceptualization, Visualization, Writing - Review & editing, Supervision.

Funding

This research did not receive any specific grant from funding agencies in the public, commercial, or not-for-profit sectors.

Declaration of Competing Interest

The authors declare that they have no known competing financial interests or personal relationships that could have appeared to influence the work reported in this paper.

Data Statement

The data on which this article is based are available in the cited literature.

References

Abt, S. R., Wittler, R. J., Taylor, A., Love, D. J., 1989. Human stability in a high flood hazard zone. Journal of the American Water Resources Association, 25(4), 881–890. https://doi.org/10.1111/j.1752-1688.1989.tb05404.x

AIDR, 2017. Flood Hazard. Australian Disaster Resilience Handbook Collection. Guideline 7-3.

Amadio, M., Scorzini, A. R., Carisi, F., Essenfelder, A. H., Domeneghetti, A., Mysiak, J., Castellarin, A., 2019. Testing empirical and synthetic flood damage models: the case of Italy, Natural Hazards and Earth System Sciences, 19, 661–678. https://doi.org/10.5194/nhess-19-661-2019

Apel, H., Aronica, G. T., Kreibich, H., Thieken, A. H., 2009. Flood risk analyses - How detailed do we need to be? Natural Hazards, 49(1), 79–98. https://doi.org/10.1007/s11069-008-9277-8

Apel, H., Thieken, A. H., Merz, B., Blöschl, G., 2004. Flood risk assessment and associated uncertainty, Natural Hazards and Earth System Sciences, 4, 295–308. https://doi.org/10.5194/nhess-4-295-2004

Arrighi, C., Alcèrreca-Huerta, J. C., Oumeraci, H., Castelli, F., 2015. Drag and lift contribution to the incipient motion of partly submerged flooded vehicles. Journal of Fluids and Structures, 57, 170–184. https://doi.org/10.1016/j.jfluidstructs.2015.06.010

Arrighi, C., Oumeraci, H., Castelli, F., 2017. Hydrodynamics of pedestrians' instability in floodwaters. Hydrology and Earth System Sciences, 21(1), 515–531. https://doi.org/10.5194/hess-21-515-2017

Arrighi, C., Mazzanti, B., Pistone, F., Castelli, F., 2020. Empirical flash flood vulnerability functions for residential buildings. SN Applied Sciences, 2, 904. https://doi.org/10.1007/s42452-020-2696-1

Aureli, F., Mignosa, P., Ziveri, C., Maranzoni, A., 2008. 2D numerical modeling for hydraulic hazard assessment: A dam-break case study. Proc., Int. Conf. Fluvial Hydraulics, River Flow 2008, 729–736.

Balica, S.F., Popescu, I., Beevers, L., Wright, N.G., 2013. Parametric and physically based modelling techniques for flood risk and vulnerability assessment: A comparison. Environmental Modelling Software, 41, 84–92. https://doi.org/10.1016/j.envsoft.2012.11.002

Bignami, D. F., Rosso, R., Sanfilippo, U., 2019. Flood Proofing in Urban Areas, first ed. Springer, Cham. https://doi.org/10.1007/978-3-030-05934-7

Black, R., 1975. Flood Proofing Rural Residences. Pennsylvania, Economic Development Administration, Washington DC: A Project Agnes Report.

Bocanegra, R. A., Vallés-Morán, F. J., Francés, F., 2020. Review and analysis of vehicle stability models during floods and proposal for future improvements. Journal of flood risk management, 13, e12551. https://doi.org/10.1111/jfr3.12551

Bonham, A. J., Hattersley, R. T., 1967. Low Level Causeways. Water Research Laboratory, The University of New South Wales, Australia, Sidney.

BWW, BRP, BUWAL, 2008. Consideration of Flood Hazard for Activities with Spatial Impact, Federal Office for the Environment, Bern, Switzerland.

Cammerer, H., Thieken, A. H., and Lammel, J., 2013. Adaptability and transferability of flood loss functions in residential areas, Natural Hazards and Earth System Sciences, 13, 3063–3081. https://doi.org/10.5194/nhess-13-3063-2013

Cardona, O., 2004. The Need for Rethinking the Concepts of Vulnerability and Risk from a Holistic Perspective: A Necessary Review and Criticism for Effective Risk Management. Mapping vulnerability. Disasters, development and people, 2003, Earthscan Publishers, London.

Cardona, O., Aalst, M., Birkmann, J., Fordham, M., Mcgregor, G., Perez, R., Pulwarty, R., Schipper, L., Sinh, B., 2012. Determinants of risk: Exposure and vulnerability. Managing the Risks of Extreme Events and Disasters to Advance Climate Change Adaptation. A Special Report of Working Groups I and II of the Intergovernmental Panel on Climate Change (IPCC). Cambridge University Press, Cambridge, UK, and New York, NY, USA, pp. 65-108.

Carisi, F., Schröter, K., Domeneghetti, A., Kreibich, H., Castellarin, A., 2018. Development and assessment of uni- and multivariable flood loss models for Emilia-Romagna (Italy). Natural Hazards and Earth System Sciences, 18(7), 2057–2079. https://doi.org/10.5194/nhess-18-2057-201

Chanson, H., Brown, R., 2015. New criterion for the stability of a human body in floodwaters. Journal of Hydraulic Research, 53(4), 540–542. https://doi.org/10.1080/00221686.2015.1054321

Chanson, H., Brown, R., 2018. Stability of Individuals during Urban Inundations: What Should We Learn from Field Observations? Geosciences, 8(9), 341. https://doi.org/10.3390/geosciences8090341

Chen, A.S., Hammond, M.J., Djordjević, S., Butler, D., Khan, D.M., Veerbeek, W., 2016. From hazard to impact: flood damage assessment tools for mega cities. Natural Hazards, 82, 857–890. https://doi.org/10.1007/s11069-016-2223-2

Chen, W., Wang, X., Deng, S., Liu, C., Xie, H., Zhu, Y., 2019. Integrated urban flood vulnerability assessment using local spatial dependence-based probabilistic approach. Journal of Hydrology 575, 454–469. https://doi.org/10.1016/j. jhydrol.2019.05.043

Clausen, L., Clark, P., 1990. The development of criteria for predicting dam break flood damages using modeling of historical dam failures. In W. White (Ed.), Proceedings of the International Conference on River Flood Hydraulics (pp. 369–380). Chichester, UK: John Wiley.

Costabile, P., Costanzo, C., De Lorenzo, G., Macchione, F., 2020. Is local flood hazard assessment in urban areas significantly influenced by the physical complexity of the hydrodynamic inundation model? Journal of Hydrology, 580, 124231. https://doi.org/10.1016/j.jhydrol.2019.124231

Cox, R. J., Shand, T. D., Blacka, M. J., 2010. Australian Rainfall and Runoff (AR&R). Revision Project 10: Appropriate Safety Criteria for People.

Dale, K., Edwards, M., Middelmann, M., Zoppou C., 2004. Structural flood vulnerability and the Australianisation of Black's curves. Risk 2004 conference proceedings. Risk Engineering Society, 8–10 November 2004, Melbourne, 2004.

Dang, N.M., Babel, M.S. Luong, H.T., 2011. Evaluation of food risk parameters in the Day River Flood Diversion Area, Red River Delta, Vietnam. Natural Hazards 56, 169–194. https://doi.org/10.1007/s11069-010-9558-x

De Moel, H., van Alphen, J., and Aerts, J. C. J. H., 2009. Flood maps in Europe – methods, availability and use, Natural Hazards and Earth System Sciences, 9, 289–301. https://doi.org/10.5194/nhess-9-289-2009

De Moel, H., Aerts, J.C.J.H., 2011. Effect of uncertainty in land use, damage models and inundation depth on flood damage estimates. Natural Hazards 58(1), 407–425. https://doi.org/10.1007/s11069-010-9675-6

De Moel, H., Jongman, B., Kreibich, H., Merz, B., Penning-Rowsell, E., Ward, P. J., 2015. Flood risk assessments at different spatial scales. Mitigation and Adaptation Strategies for Global Change, 20, 865–890. https://doi.org/10.1007/s11027-015-9654-z

De Risi, R., Jalayer, F., De Paola, F., Iervolino, I., Giugni, M., Topa, M. E., Mbuya, E., Kyessi, A., Manfredi, G., Gasparini, P., 2013. Flood risk assessment for informal settlements. Natural Hazards, 69,1003–1032. https://doi.org/10.1007/s11069-013-0749-0

Dottori, F., Figueiredo, R., Martina, M. L. V., Molinari, D., Scorzini, A. R., 2016. INSYDE: A synthetic, probabilistic flood damage model based on explicit cost analysis. Natural Hazards and Earth System Sciences, 16(12), 2577–2591. https://doi.org/10.5194/nhess-16-2577-2016

Dutta, D., Herath, S., Musiake, K., 2003. A mathematical model for flood loss estimation. Journal of Hydrology, 277 (1-2), 24–49. https://doi.org/10.1016/S0022-1694(03)00084-2

Ettinger, S., Mounaud, L., Magill, C., Yao-Lafourcade, A.F., Thouret, J.C., Manville, V., Negulescu, C., Zuccaro, G., De Gregorio, D., Nardone, S., Uchuchoque, J.A.L., Arguedas, A., Macedo, L., Llerena, N.M., 2016. Building vulnerability to hydro-geomorphic hazards: estimating damage probability from qualitative vulnerability assessment using logistic regression. Journal of Hydrology. 541 (Part A), 563–581. https://doi.org/10.1016/j.jhydrol.2015.04.017

Ferrari, A., Viero, D. P., Vacondio, R., Defina, A., Mignosa, P., 2019. Flood inundation modeling in urbanized areas: A mesh-independent porosity approach with anisotropic friction. Advances in water resources, 125, 98-113. https://doi.org/10.1016/j.advwatres.2019.01.010

Ferrari, A., Dazzi, S., Vacondio, R., Mignosa, P., 2020. Enhancing the resilience to flooding induced by levee breaches in lowland areas: a methodology based on numerical modelling. Natural Hazards and Earth System Sciences, 20(1), 59–72. https://doi.org/10.5194/nhess-20-59-2020

Ferrari, A., Viero, D. P., 2020. Floodwater pathways in urban areas: A method to compute porosity fields for anisotropic subgrid models in differential form. Journal of Hydrology, 589, 125193. https://doi.org/10.1016/j.jhydrol.2020.125193

Foster, D. N., Cox, R., 1973. Stability of children on roads used as floodways, Tech. Rep. 73/13, Univ. of N. S. W., Water Res. Lab., Sidney, Australia.

Fuchs, S., Keiler, M., Ortlepp, R., Schinke, R., Papathoma-Köhle, M., 2019a. Recent advances in vulnerability assessment for the built environment exposed to torrential hazards: Challenges and the way forward. Journal of Hydrology, 575, 587–595. https://doi.org/10.1016/j.jhydrol.2019.05.067

Fuchs, S., Heiser, M., Schlögl, M., Zischg, A., Papathoma-Köhle, M., Keiler, M., 2019b. Short communication: A model to predict flood loss in mountain areas. Environmental Modelling & Software, 117, 176–180. https://doi.org/10.1016/j.envsoft.2019.03.026

Gallegos, H. A., Schubert, J. E., Sanders, B. F., 2012. Structural Damage Prediction in a High-Velocity Urban Dam-Break Flood: Field-Scale Assessment of Predictive Skill. Journal of Engineering Mechanics, 138, 10, 1249-1262. https://doi.org/10.1061/(ASCE)EM.1943-7889.0000427

Garrote, J., Alvarenga, F.M., Díez-Herrero A., 2016. Quantification of flash flood economic risk using ultra-detailed stage–damage functions and 2-D hydraulic models. Journal of Hydrology, 541, 611-625, https://doi.org/10.1016/j.jhydrol.2016.02.006

Gems, B., Mazzorana, B., Hofer, T., Sturm, M., Gabl, R., Aufleger, M., 2016. 3-D hydrodynamic modelling of flood impacts on a building and indoor flooding processes, Natural Hazards and Earth System Sciences, 16, 1351–1368. https://doi.org/10.5194/nhess-16-1351-2016

Gerl, T., Kreibich, H., Franco, G., Marechal, D., Schröter, K., 2016. A Review of Flood Loss Models as Basis for Harmonization and Benchmarking. PLOS ONE, 11(7), e0159791. https://doi.org/10.1371/journal.pone.0159791

Gordon, A. D., Stone, P. B., 1973. Car Stability on Road Causeways. Water Research Laboratory, The University of New South Wales, Manly Vale, NSW, Australia, Technical Report No. 73/12.

Gumière, S. J., Camporese, M., Botto, A., Lafond, J. A., Paniconi, C., Gallichand, J., Rousseau, A. N., 2020. Machine Learning vs. Physics-Based Modeling for Real-Time Irrigation Management. Frontiers in Water, 2,8. https://doi.org/10.3389/frwa.2020.00008

Hammond, M., Chen, A., Djordjević, S., Butler, D., Mark, O., 2015. Urban flood impact assessment: A state-of-the-art review. Urban Water Journal, 12, 14-29. https://doi.org/10.1080/1573062X.2013.857421

Hasanzadeh Nafari, R., Amadio, M., Ngo, T., Mysiak, J., 2017. Flood loss modelling with FLF-IT: A new flood loss function for Italian residential structures. Natural Hazards and Earth System Sciences, 17(7), 1047–1059. https://doi.org/10.5194/nhess-17-1047-2017

Haugen, E.D., Kaynia, A.M., 2008. Vulnerability of structures impacted by debris flow. In: Landslides and Engineered Slopes. From the Past to the Future, Two Volumes + CD-ROM, first ed. CRC Press, ISBN: 9780429207242.

Huizinga, J., de Moel, H., Szewczyk, W., 2017. Global flood depth-damage functions: Methodology and the Database with Guidelines, JRC Technical Reports. https://doi.org/10.2760/16510

ISTAT, 2020. Annuario statistico italiano - 2020. Istituto nazionale di statistica, ISBN 978-88-458-2035-9.

Jamali, B., Löwe, R., Bach, P. M., Urich, C., Arnbjerg-Nielsen, K., Deletic, A., 2018. A rapid urban flood inundation and damage assessment model, Journal of Hydrology, 564, 1085–1098. https://doi.org/10.1016/j.jhydrol.2018.07.064

Jongman, B., Kreibich, H., Apel, H., Barredo, J. I., Bates, P. D., Feyen, L., Gericke, A., Neal, J., Aerts, J. C. J. H., Ward, P. J., 2012. Comparative flood damage model assessment: Towards a European approach. Natural Hazards and Earth System Science, 12(12), 3733–3752. https://doi.org/10.5194/nhess-12-3733-2012

Jonkman, S. N., Penning-Rowsell, E., 2008. Human instability in flood flows. Journal of the American Water Resources Association, 44(5), 1208–1218. https://doi.org/10.1111/j.1752-1688.2008.00217.x

Karagiorgos, K., Thaler, T., Heiser, M., Hübl, J.,Fuchs, S., 2016. Integrated flash flood vulnerability assessment: Insights from East Attica, Greece. Journal of Hydrology, 541, 553-562. https://doi.org/10.1016/j.jhydrol.2016.02.052

Karvonen, R. A., Hepojoki, H. K., Huhta, H. K., Louhio, A., 2000. The Use Of Physical Models In Dam-Break Flood Analysis, Development of rescue actions based on dam-break flood analysis (RESCDAM). Final report of Helsinki University of Technology.

Keller, R. J., Mitsch, B., 1993. Safety Aspects of the Design of Roadways as Floodways. Research Report No. 69, Urban Water Research Association of Australia.

Kellermann, P., Schöbel, A., Kundela, G., Thieken, A. H., 2015. Estimating flood damage to railway infrastructure – the case study of the March River flood in 2006 at the Austrian Northern Railway, Natural Hazards and Earth System Sciences, 15, 2485–2496, https://doi.org/10.5194/nhess-15-2485-2015

Kelman, O., Spence, R., 2004. An overview of flood actions on buildings. Engineering Geology, 73, 297–309. https://doi.org/10.1016/j.enggeo.2004.01.010

Kok, M., Huizinga, H. J., Barendregt, A., 2005. Standard Method 2004: Damage and Casualties Caused by Flooding.

Koks, E. E., Bočkarjova, M., de Moel, H., Aerts, J. C., 2015. Integrated direct and indirect flood risk modeling: development and sensitivity analysis. Risk analysis, 35(5), 882-900. https://doi.org/10.1111/risa.12300

Kramer, M., Terheiden, K., Wieprecht, S., 2016. Safety criteria for the trafficability of inundated roads in urban floodings. International Journal of Disaster Risk Reduction, 17(April), 77–84. https://doi.org/10.1016/j.ijdrr.2016.04.003

Kreibich, H., Piroth, K., Seifert, I., Maiwald, H., Kunert, U., Schwarz, J., Merz, B., Thieken, A. H., 2009. Is flow velocity a significant parameter in flood damage modelling? Natural Hazards and Earth System Sciences, 9(5), 1679–1692. https://doi.org/10.5194/nhess-9-1679-2009

Kreibich, H., Botto, A., Merz, B., and Schröter, K., 2017. Probabilistic, multivariable flood loss modeling on the mesoscale with BT-FLEMO, Risk Analysis, 37, 774–787, https://doi.org/10.1111/risa.12650

Krzysztofowicz, R., Davis, D. R., 1983. Category-unit loss functions for flood forecast-response system evaluation. Water Resources Research, 19(6), 1476–1480. https://doi.org/10.1029/WR019i006p01476

Kvocka, D., Falconer, R. A., Bray, M., 2016. Flood hazard assessment for extreme flood events. Natural Hazards, 84, 1569–1599. https://doi.org/10.1007/s11069-016-2501-z

Lacasta, A., Morales-Hernández, M., Murillo, J., García-Navarro, P., 2014. An optimized GPU implementation of a 2D free surface simulation model on unstructured meshes. Advances in engineering software, 78, 1-15. https://doi.org/10.1016/j.advengsoft.2014.08.007

Leelawat, N., Suppasri, A., Charvet, I., Imamura, F., 2014. Building damage from the 2011 Great East Japan tsunami: Quantitative assessment of influential factors: A new perspective on building damage analysis. Natural Hazards, 73(2), 449–471. https://doi.org/10.1007/s11069-014-1081-z

Lind, N., Hartford, D., Assaf, H., 2004. Hydrodynamic Models of Human Instability in a Flood. Journal of the American Water Resources Association, 40(1), 89–96 https://doi.org/10.1111/j.1752-1688.2004.tb01012.x

Lv, H., Wu, Z., Guan, X., Meng, Y., 2021. The construction of flood loss ratio function in cities lacking loss data based on dynamic proportional substitution and hierarchical Bayesian model. Journal of Hydrology, 592, 125797. https://doi.org/10.1016/j.jhydrol.2020.125797

Maiwald, H., Schwarz, J., 2015. Damage and loss prognosis tools correlating flood action and building's resistance-type parameters. International Journal of Safety and Security Engineering. 5. 222-250. https://doi.org/10.2495/SAFE-V5-N3-222-250

Martínez-Gomariz, E., Gómez, M., Russo, B., 2016. Experimental study of the stability of pedestrians exposed to urban pluvial flooding. Natural Hazards, 82(2), 1259–1278. https://doi.org/10.1007/s11069-016-2242-z

Martínez-Gomariz, E., Gómez, M., Russo, B., Djordjević, S., 2018. Stability criteria for flooded vehicles: A state-of-the-art review. Journal of Flood Risk Management, 11, S817–S826. https://doi.org/10.1111/jfr3.12262

Martínez-Gomariz, E., Gómez, M., Russo, B., Sánchez, P., Montes, J. A., 2019. Methodology for the damage assessment of vehicles exposed to flooding in urban areas. Journal of Flood Risk Management, 12(3), e12475–e12475. https://doi.org/10.1111/jfr3.12475

Martínez-Gomariz, E., Forero-Ortiz, E., Russo, B., Locatelli, L., Guerrero-Hidalga, M., Yubero, D., Castan, S., 2021. A novel expert opinion-based approach to compute estimations of flood damage to property in dense urban environments. Barcelona case study, Journal of Hydrology, 598, 126244. https://doi.org/10.1016/j.jhydrol.2021.126244

Mazzorana, B., Simoni, S., Scherer, C., Gems, B., Fuchs, S., and Keiler, M., 2014. A physical approach on flood risk vulnerability of buildings, Hydrology and Earth System Sciences, 18, 3817–3836. https://doi.org/10.5194/hess-18-3817-2014

McBean, E. A., Gorrie, J., Fortin, M., Ding, J., Moulton, R., 1988. Adjustment factors for flood damage curves. Journal of Water Resources Planning and Management, 114(6), 635–646. https://doi.org/10.1061/(ASCE)0733-9496(1988)114:6(635)

McGrath, H., El Ezz, A. A., Nastev, M., 2019. Probabilistic depth–damage curves for assessment of flood-induced building losses. Natural Hazards, 97(1), 1–14. https://doi.org/10.1007/s11069-019-03622-3

Menoni, S., Molinari, D., Parker, D., Ballio, F., Tapsell, S., 2012. Assessing multifaceted vulnerability and resilience in order to design risk-mitigation strategies. Natural Hazards, 64, 2057–2082. https://doi.org/10.1007/s11069-012-0134-4

Merz, B., Kreibich, H., Lall, U., 2013. Multi-variate flood damage assessment: A tree-based data-mining approach. Natural Hazards and Earth System Sciences, 13(1), 53–64. https://doi.org/10.5194/nhess-13-53-2013

Merz, B., Kreibich, H., Schwarze, R., Thieken, A., 2010. Assessment of economic flood damage. Natural Hazards and Earth System Sciences, 10(8), 1697–1724. https://doi.org/10.5194/nhess-10-1697-2010

Merz, B., Kreibich, H., Thieken, A., Schmidtke, R., 2004. Estimation uncertainty of direct monetary flood damage to buildings. Natural Hazards and Earth System Sciences, 4(1), 153–163. https://doi.org/10.5194/nhess-4-153-2004

Middelmann-Fernandes, M. H., 2010. Flood damage estimation beyond stage–damage functions: an Australian example. Journal of Flood Risk Management, 3, 88–96. https://doi.org/10.1111/j.1753-318X.2009.01058.x

Mignot, E., Li, X., Dewals, B., 2019. Experimental modelling of urban flooding: A review. Journal of Hydrology, 568, 334-342. https://doi.org/10.1016/j.jhydrol.2018.11.001

Milanesi, L., Pilotti, M., 2019. A conceptual model of vehicles stability in flood flows. Journal of Hydraulic Research, 1–8. https://doi.org/10.1080/00221686.2019.1647887

Milanesi, L., Pilotti, M., Bacchi, B., 2016. Using web-based observations to identify thresholds of a person's stability in a flow. Water Resources Research, 52(10), 7793–7805. https://doi.org/10.1002/2016WR019182

Milanesi, L., Pilotti, M., Belleri, A., Marini, A., Fuchs, S., 2018. Vulnerability to flash floods: A simplified structural model for masonry buildings. Water Resources Research, 54, 7177– 7197. https://doi.org/10.1029/2018WR022577

Milanesi, L., Pilotti, M., Ranzi, R., 2015. A conceptual model of people's vulnerability to floods. Water Resources Research, 51(1), 182–197. https://doi.org/10.1002/2014WR016172

Molinari, D., Ballio, F., Handmer, J., Menoni, S., 2014. On the modeling of significance for flood damage assessment. International Journal of Disaster Risk Reduction, 10, 381–391. https://doi.org/10.1016/j.ijdrr.2014.10.009

Molinari, D., Scorzini, A.R., 2017. On the influence of input data quality to flood damage estimation: the performance of the INSYDE model. Water, 9, 688. https://doi.org/10.3390/w9090688

Molinari, D., De Bruijn, K., Castillo, J., Aronica, G., Bouwer, L., 2019. Validation of flood risk models: Current practice and possible improvements. International Journal of Disaster Risk Reduction, 33. https://doi.org/10.1016/j.ijdrr.2018.10.022

Molinari, D., Scorzini, A. R., Arrighi, C., Carisi, F., Castelli, F., Domeneghetti, A., Gallazzi, A., Galliani, M., Grelot, F., Kellermann, P., Kreibich, H., Mohor, G. S., Mosimann, M., Natho, S., Richert, C., Schroeter, K., Thieken, A. H., Zischg, A. P., Ballio, F., 2020. Are flood damage models converging to "reality"? Lessons learnt from a blind test, Natural Hazards and Earth System Sciences, 20, 2997–3017. https://doi.org/10.5194/nhess-20-2997-2020

Mosavi A, Ozturk P, Chau K. W., 2018. Flood Prediction Using Machine Learning Models: Literature Review. Water, 10(11):1536. https://doi.org/10.3390/w10111536

Nadal, N. C., Zapata, R. E., Pagán, I., López, R., Agudelo, J., 2010. Building Damage due to Riverine and Coastal Floods. Journal of Water Resources Planning and Management, 136, 3, 327-336. https://doi.org/10.1061/(ASCE)WR.1943-5452.0000036

Nofal, O. M., van de Lindt, J. W., Do, T. Q., 2020. Multi-variate and single-variable flood fragility and loss approaches for buildings. Reliability Engineering System Safety, 202(106971) https://doi.org/10.1016/j.ress.2020.106971

Oshikawa, H., Oshima, T., Komatsu, T., 2011. Study on the Risk for Vehicular Traffic in a Flood Situation (in Japanese). Advances in River Engineering JSCE, 17, 461–466.

Papathoma-Köhle, M., Gems, B., Sturm, M., Fuchs, S., 2017. Matrices, curves and indicators: A review of approaches to assess physical vulnerability to debris flows. Earth-Science Reviews, 171,272-288. https://doi.org/10.1016/j.earscirev.2017.06.007

Papathoma-Köhle, M., Schlögl, M., Fuchs, S., 2019. Vulnerability indicators for natural hazards: an innovative selection and weighting approach. Scientific Reports, 9, 15026. https://doi.org/10.1038/s41598-019-50257-2

Penning-Rowsell, E., Floyd, P., Ramsbottom, D., Surendran, S., 2005. Estimating injury and loss of life in floods: A deterministic framework. Natural Hazards, 36(1–2), 43–64. https://doi.org/10.1007/s11069-004-4538-7

Pham, B.T., Luu, C., Van Phong, T., Nguyen, H.D., Van Le, H., Tran, T.Q., Ta, H.T., Prakash, I., 2020. Flood risk assessment using hybrid artificial intelligence models integrated with multi-criteria decision analysis in Quang Nam Province, Vietnam. Journal of Hydrology, 125815 https://doi.org/10.1016/j.jhydrol.2020.125815

Postacchini, M., Zitti, G., Giordano, E., Clementi, F., Darvini, G., Lenci, S., 2019. Flood impact on masonry buildings: The effect of flow characteristics and incidence angle. Journal of Fluids and Structures, 88, 48-70. https://doi.org/10.1016/j.jfluidstructs.2019.04.004

Postacchini, M., Bernardini, G., D'Orazio, M., Quagliarini, E., 2021. Human stability during floods: Experimental tests on a physical model simulating human body. Safety Science, 137, 105153. https://doi.org/10.1016/j.ssci.2020.105153

Pistrika, A.K., Jonkman, S.N., 2009. Damage to residential buildings due to flooding of New Orleans after hurricane Katrina. Natural Hazards 54(2), 413–434. https://doi.org/10.1007/s11069-009-9476-y

Pita, G. L., Albornoz, B. S., Zaracho, J. I., 2021. Flood depth-damage and fragility functions derived with structured expert judgment. Journal of Hydrology, 603, 126982. https://doi.org/10.1016/j.jhydrol.2021.126982

Pregnolato, M., Galasso, C., Parisi, F., 2015. A compendium of existing vulnerability and fragility relationships for flood: Preliminary results. Proc., 12th Int. Conf. on Applications of Statistics and Probability in Civil Engineering, ICASP12, 1–8, Los Angeles: Civil Engineering Risk and Reliability Association.

Ramsbottom, D., Wade, S., Bain, V., 2006. Flood Risks to People—Phase 2—FD2321/TR2 Guidance Document. Flood Hazard Research Centre, Middlesex University.

Roos, W., Waarts, P., Vrouwenvelder, A., 2003. Damage to buildings. Delft Cluster paper, DC1-233–9, 1–45.

Russo, B., Gómez, M., Macchione, F., 2013. Pedestrian hazard criteria for flooded urban areas. Natural Hazards, 69(1), 251–265. https://doi.org/10.1007/s11069-013-0702-2

Sanders, B. F., Schubert, J. E., 2019. PRIMo: Parallel raster inundation model. Advances in Water Resources, 126, 79-95. https://doi.org/10.1016/j.advwatres.2019.02.007

Schröter, K., Kreibich, H., Vogel, K., Riggelsen, C., Scherbaum, F., and Merz, B., 2014. How useful are complex flood damage models?, Water Resources Research, 50, 3378– 3395. https://doi.org/10.1002/2013WR014396

Scorzini, A. R., Frank, E., 2017. Flood damage curves: New insights from the 2010 flood in Veneto, Italy. Journal of Flood Risk Management, 10(3), 381–392. https://doi.org/10.1111/jfr3.12163

Shand, T. D., Cox, R. J., Blacka, M. J., Smith, G. P., 2011. Australian rainfall and runoff (AR&R). Revision project 10: Appropriate safety criteria for vehicles. Report Number: P10/S2/020.

Shu, C., Xia, J., Falconer, R. A., Lin, B., 2011. Incipient velocity for partially submerged vehicles in floodwaters. Journal of Hydraulic Research, 49(6), 709–717. https://doi.org/10.1080/00221686.2011.616318

Smith, D. I., 1994. Flood damage estimation. A review of urban stage damage curves and loss functions. Water South Africa, 20(3), 231–238. https://doi.org/10520/AJA03784738_1124

Smith, G.P., Davey, E.K., Cox, R.J., 2014. Flood hazard. Technical report 2014/07, Water Research Laboratory, University of New South Wales, Sydney.

Smith, G. P., Modra, B. D., Felder, S., 2019. Full-scale testing of stability curves for vehicles in flood waters. Journal of Flood Risk Management, 12, 1–15. https://doi.org/10.1111/jfr3.12527

Takahashi, S., Endoh, K., Muro, Z. I., 1992. Experimental study on people's safety against overtopping waves on breakwaters. Rep. 31-04, The Port and Harbour Res. Inst., Yokosuka, Japan.

Teo, F. Y., Xia, J., Falconer, R. A., Lin, B., 2012. Experimental studies on the interaction between vehicles and floodplain flows. International Journal of River Basin Management, 10, 149–160. https://doi.org/10.1080/15715124.2012.674040

Thapa, S., Shrestha, A., Lamichhane, S., Adhikari, R., Gautam, D., 2020. Catchment-scale flood hazard mapping and flood vulnerability analysis of residential buildings: The case of Khando River in eastern Nepal, Journal of Hydrology: Regional Studies, 30, 100704. https://doi.org/10.1016/j.ejrh.2020.100704

Thieken, A. H., Müller, M., Kreibich, H., and Merz, B., 2005. Flood damage and influencing factors: New insights from the August 2002 flood in Germany, Water Resources Research, 41, W12430. https://doi.org/10.1029/2005WR004177

Thieken, A. H., Olschewski, A., Kreibich, H., Kobsch, S., Merz, B., 2008. Development and evaluation of FLEMOps—A new Flood Loss Estimation MOdel for the private sector. WIT Transactions on Ecology and the Environment, 118, 315–324. https://doi.org/10.2495/FRIAR080301

Thywissen, K., 2006. Core terminology of disaster reduction: A comparative glossary. Measuring Vulnerability to Natural Hazards, UNU-Press, Tokyo, Japan, 448–496.

Toda, K., Ishigaki, T., Ozaki, T., 2013. Experiments study on floating car in flooding. International Conference on Flood Resilience: Experiences in Asia and Europe (Vol. 6).

Van Ootegem, L., Verhofstadt, E., Van Herck, K., Creten, T., 2015. Multivariate pluvial flood damage models. Environmental Impact Assessment Review, 54, 91–100. https://doi.org/10.1016/j.eiar.2015.05.005

Van Ootegem, L., Van Herck, K., Creten, T., Verhofstadt, E., Foresti, L., Goudenhoofdt, E., Reyniers, M., Delobbe, L., Murla Tuyls, D., Willems, P., 2018. Exploring the potential of multivariate depth-damage and rainfall-damage models. Journal of Flood Risk Management, 11(S2), S916–S929. https://doi.org/10.1111/jfr3.12284

Wang, Z., Lai, C., Chen, X., Yang, B., Zhao, S., Bai., 2015. Flood hazard risk assessment model based on random forest. Journal of Hydrology, 527, 1130-1141. https://doi.org/10.1016/j.jhydrol.2015.06.008

Wang, Y., Marsooli, R., 2021. Physical instability of individuals exposed to storm-induced coastal flooding: Vulnerability of New Yorkers during Hurricane Sandy. Water Resources Research, 57, e2020WR028616. https://doi.org/10.1029/2020WR028616

Xia, J., Falconer, R. A., Wang, Y., Xiao, X., 2014a. New criterion for the stability of a human body in floodwaters. Journal of Hydraulic Research, 52, 93–104. https://doi.org/10.1080/00221686.2013.875073

Xia, J., Falconer, R. A., Xiao, X., Wang, Y., 2014b. Criterion of vehicle stability in floodwaters based on theoretical and experimental studies. Natural Hazards, 70, 1619–1630. https://doi.org/10.1007/s11069-013-0889-2

Xia, J., Teo, F. Y., Lin, B., Falconer, R. A., 2011. Formula of incipient velocity for flooded vehicles. Natural Hazards, 58(1), 1–14. https://doi.org/10.1007/s11069-010-9639-x

Yee, M., 2003. Human stability in floodways. Undergraduate Honours Thesis - School of Civil and Environmental Engineering, University of New South Wales, Sydney, Australia.

Zhou, Q., Mikkelsen, P.S., Halsnæs, K., Arnbjerg-Nielsen, K., 2012. Framework for economic pluvial flood risk assessment considering climate change effects and adaptation benefits, Journal of Hydrology, 414–415, 539–549. https://doi.org/10.1016/j.jhydrol.2011.11.031